2 Chapter: Identification of Phytoestrogens as Sirtuin Inhibitor Against Breast Cancer: Multitargeted Approach

2.1 Introduction:

Cancer is a heterogeneous disease characterized by abnormal growth and uncontrolled proliferation of cells which sometimes invade the surrounding tissues and metastasize to distinct body sites. Out of cancers of all different types, lungs, skin, and breast cancer are the most prevalent ones [96]. The most common cancer in women is breast cancer, and its prevalence is increasing globally with around 2.3 million new cases annually [97]. Breast cancer is the second most cause of death among females, affecting around 0.6 million especially in Europe [98]. Breast cancer can be treated using various treatment approaches including chemotherapy, surgical interventions, radiation therapy, hormonal therapy, immune therapy. However, the side effect profile and drug resistance potential of currently available therapies limit their application. Therefore, researchers are investigating novel molecular targets to treat aggressive and advanced breast cancers [99]. In the development of various cancers, including breast, colon, head and neck, lung, and ovarian cancer. sirtuins are considered a major therapeutic target due to their role both as tumor promoters and tumor suppressors [100].

Sirtuins (SIRT) are uniformly and differentially expressed in the nuclear portion (SIRT-1, 6, and 7), the mitochondrial section (SIRT3, 4, and 5), and the cytoplasm (SIRT2) of diverse tissues [101]. The conserved catalytic core domain of sirtuins is surrounded by flexible N- and C-terminal extensions that can affect their cellular location, substrate selectivity, and enzymatic activity [102]. The core domain normally has 275 amino acids and consist of the NAD+-binding Rossmann Fold Domain is necessary for the deacetylation process, and Zinc-Binding Domain essential for preserving the protein's structural integrity as it coordinates a zinc ion through conserved cysteine residues [103]. Sirtuins assume a closed conformation, a catalytic loop, and stabilize the reductions that

are engaged in catalysis when they are in the active state [104]. On the other hand, in the inactive state, the key reduces, the catalytic loop is displaced, and the open loop is formed [105].

SIRT-1 overexpression in breast cancer cells is known to increase the multidrug resistant mutation 1 gene which prevents build-up of chemotherapeutic drugs inside the cells [106, 107]. The downregulation of SIRT-1 causes β-catenin and c-Jun to be less abundant further leading to decline in expression of Frizzled 7 gene [108]. Furthermore, patient-derived breast cancer tissue samples showed that SIRT-1 plays a critical role in upregulating MMP-2 protein levels through its deacetylation activity leading to poor patient survival rate [108]. In estrogen receptor-negative breast cancers, increased nuclear SIRT2 amplification is associated with a shorter time to recurrence and greater rates of disease-specific mortality [109]. When SIRT-1 is inhibited, heat shock factor 1 (HSF1) is downregulated which in turn, speeds up the downregulation of multidrug resistance (MDR) associated P-gp protein causing reduction in MDR breast cancer cells [110]. Tamoxifen resistance in estrogen receptor-alpha (ER-α) positive breast cancer cells is partly attributed to SIRT-1, which promotes the deacetylation of FoxO1 protein and consequent up-regulation of MDR protein 2 [107]. SIRT1-deficient cells showed downregulation of MDR1 and enhanced ionizing radiation-induced thymocyte death in vivo, as well as p53 hyperacetylation after DNA damage [111].

Hormone receptor-positive breast cancer cells with silenced SIRT3 gene showed impaired antioxidant response causing enhanced susceptibility to cisplatin and tamoxifen [112].The expression of SIRT3 in breast cancer cells has been linked to controlled ROS production and enhanced antioxidant activity which facilitates drug resistance [113]. Numerous signaling pathways, such as AMPK, p53, FOXO, NF-κB, HIF, PGC-1α, and

the insulin/IGF-1 pathway, are regulated by SIRT receptors, especially SIRT1 [114]. P53 is deacetylated by SIRT1, which inactivates it. When there is stress (such as DNA damage), p53 is triggered, which results in apoptosis or cell cycle arrest [115]. By deacetylating p53 through SIRT1, cell survival during stress is increased [56]. All of these pathways have an impact on many cellular functions, including mitochondrial function, metabolism, stress response, inflammation, and apoptosis. Therefore, the development of dual inhibitors that target both SIRT1 and SIRT3 proteins could be a potential therapeutic option in the treatment of cancer [100].

Numerous synthetic SIRT inhibitors have been developed in order to effectively inhibit sirtuins, and consequently, the process of tumorigenesis [116]. However, the phytoestrogens exhibiting structural and physiological similarities with endogenous estrogens of humans [117, 118] are not extensively studied for their sirtuin inhibition property and subsequent anticancer activity. Apparently, there is lack of much research done on phytoestrogens stability, and binding affinity within the binding sites of different SIRT isoforms. Therefore, the current study considered ten different phytoestrogens (apigenin, coumestrol, cynadine, enterolatone, epicatachine, genestine, kaempherol, narigenin, resvestrol, and xanthohumonol) with reports of anticancer activity for further evaluation [119].

Phytoestrogens may lessen the efficacy of anti-cancer treatments by controlling oxidative stress and other processes. In addition, their use may increase the risk of carcinogenesis, laid breast cancer survivors at risk of recurrence, and endanger patients [120]. Their main function is to shield cellular structures from reactive oxygen species (ROS), like epicatechin and lignans [121]. However, when they are converted into their active metabolites, enterolactone and enterodiol, their effects in vivo are much stronger

[122]. Certain findings state that excessive concentrations of phytoestrogens might have an oxidative impact and result in cell death. Many compounds, including as genistein, resveratrol, and xanthohumol, have been reported to have this activity [123]. Previous research has demonstrated that phytoestrogens exhibit higher affinity to estrogen receptors specially Erβ. Lack of ERβ has been associated with more aggressive types of breast cancer, proving that ERβ is an essential tumor suppressor gene that limits the proliferation produced by ERα [124]. This preference for binding to ERβ is important because, in contrast to the carcinogenic consequences connected to ERα signalling. The MCF-7 cells has characteristics of the luminal subtype breast tumors with a hormone-dependent (positive for both progesterone and estrogen receptors, but HER2 negative) growth and survival profile. MDA-MB-231 cells on the other hand are triple negative (ER, PR and HER2 negative) [125]. It is usual practice to model late-stage breast cancer using the MDA-MB-231 cell line, which was obtained at MD Anderson from a pleural effusion of a patient with invasive ductal carcinoma. This cell line expresses mutant p53 and is negative not only for ER, PR, HER2 but also for E-cadherin. MDA-MB-231 cells serve as a model for more aggressive, hormone-independent breast cancer [126].

The cell lines MCF-7 and MDA-MB-231 represent well-known in vitro models of breast cancer. The phenotypic and genotypic contrasts between these cells, despite their shared invasive ductal/breast carcinoma nature, make these mammalian breast cancer cells suitable for the present study, which was the rationale behind selection of these cell lines for our study. In MCF-7 cells, SIRT-1 overexpression stimulates proliferation, migration, and invasion, whereas its knockdown reduces these activities [127]. SIRT-1 expression is greater in breast cancer tissues than in non-cancerous tissues [127].

The present study was designed to evaluate the potential of phytoestrogens against SIRTs (1–3) using molecular docking studies, molecular dynamic studies, and in vitro studies. The molecular docking study was conducted to examine the binding interactions of ten known phytoestrogens against SIRTs (1–3). The phytoestrogen coumestrol was chosen for further molecular dynamic simulation to examine the stability and compatibility of coumestrol-SIRTs (1–3) complexes. The computational findings were further validated by conducting MTT assay to study effect of coumestrol on cellular viability, colony formation assay to study the consequence of coumestrol on new colony formation, flow-cytometry assay to study effect of coumestrol on the intracellular reactive oxygen species levels, and the Western blotting to assess the effect of coumestrol on expression of SIRT-1 protein in cancer cell lines. In conclusion, our combined in silico and in vitro results support the potential of phytoestrogens as therapeutic agents against SIRT-associated breast cancer.

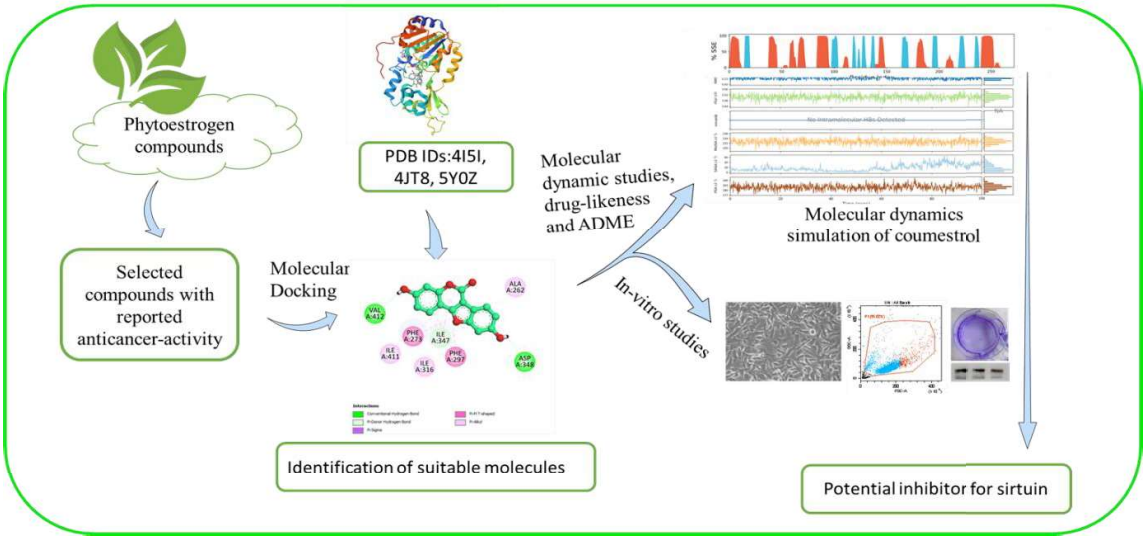

Figure 5: Graphical representation of workflow.

2.2 Materials and methods:

2.2.1 Molecular docking studies:

2.2.1.1 Preparation of Ligand library:

We made a ligand library containing 13 compounds including 10 phytoestrogens and three synthetic SIRT inhibitors. These compounds were incorporated in the library on the basis of their class and anticancer modulation properties [128-134]. From PubChem database, we retrieved the chemical structures of phytoestrogens and subsequently conducted 3D structural optimizations. The energy minimization process involved using Chem 3D 20.1.1 software to initially generate 2D representations of the ligands followed by further optimizations to enhance bond lengths and angles, thereby improving the overall ligand energies.

2.2.1.2 Protein preparation:

The crystallographic data of SIRT-1 (PDB ID: 4I5I), SIRT2 (PDB ID: 5Y0Z) and SIRT3 (PDB ID: 4JT8) [135-137] were chosen based on their improved resolution, lack of mutation, and ability to be combine for efficient similarity analysis and information of these proteins suggesting previous reports for better specific SIRT proteins [138-141] were obtained from Protein Data Bank (PDB) (https://www.rcsb.org/). Proteins were processed by eliminating water particles, non-essential atoms, and attached ligands (if any). We used the client version of Discovery Studio 2021 to create the protein structures. Afterwards, the proteins were subjected to further processing, which included adding hydrogen, eliminating alternative conformations, and adding missing atoms to incomplete residues.

2.2.1.3 Docking:

After preparing the ligand and protein libraries, AutoDock 4 [142] was utilized to perform molecular docking studies. The pre-prepared proteins and ligands were loaded into AutoDock and saved as pdbqt file format. Additionally, grid parameters were configured by targeting amino acids within the active sites; SIRT-1 Chain A: PHE119, PHE131, ALA135, ARG97, PHE190, PRO140, TYR139, ILE169, and SIRT-2 Chain A: ASP348, ILE347, ILE411, PHE297, PHE413 and SIRT-3 Chain A: ASP231, HIS248, VAL298, PHE180, ASP156, ALA146. The grid size (X:56, Y:40, Z:40) and grid position (X: 43.383, Y: -21.117, Y: 16.916) was validated for SIRT-1. And for SIRT-2, grid size (X:56, Y:50, Z:68) and grid position (X: 13.227, Y: 49.057, Z: -27.311) similarly for SIRT-3, grid size (X:40 Y:40, Z:56) and grid position (X: 24.728, Y: 43.506, Z: -10.585) were validated. The ligands and targeted proteins (SIRTs 1-3) of docking was performed by using Lamarckian genetic algorithm 4.2. after the setup of genetic algorithms to 100 runs with the default docking settings. Discovery Studio Visualizer 2021 client (BIOVIA 21.1.0) were used to analyzed the results obtained from the docking and the resulted files were documented. The docking parameters were validated using three reference compounds including EX-527 (SIRT-1 inhibitor), NPD11033 (SIRT2 inhibitor), and EX-A3489 (SIRT3 inhibitor). We have performed the docking studies using several docking algorithm platforms includes Auto dock vina and Schrödinger.

2.2.1.4 Molecular dynamic simulations of coumestrol:

The molecular dynamic studies were performed using Desmond (Maestro-Desmond) software tool. The binding interaction profile and stability of the docked ligands along with reference compounds were analyzed on the recombinant human SIRTs 1-3 (PDB ID:4I5I, 5Y0Z and 4JT8). The aqueous environment was created by positioned

TIP3P water molecule in a cubic box and the physiological cell conditions were maintained by addition of 0.15 M NaCl. Further, with a fixed temperature of 310K and set pressure of 1 bar the simulation was run under constant volume and temperature utilizing NPT ensemble conditions, further the system was cooled to allow molecular dynamic simulation. The results of 100 ns of dynamic simulations were evaluated using RMSD interaction plots formed by carbon atoms and RMSF interactions follows to understand the stability of ligand pocket binding with the help of Maestro. (Schrödinger, LLC, New York) [143].

2.2.1.5 Molecular mechanics and generalized born surface area (MM-GBSA) calculations:

During MD simulations of the SIRTs complexes bound with coumestrol, and reference compounds. By predicting the polar solvation energy, the implicit solvent model—specifically, the Generalized Born (GB) model—plays a critical role in MMGBSA computations. Important parameters in this model are the dielectric constant of the solvent and the dielectric constant of the solute. Choosing the right GB model (e.g., GBOBC1 or GBOBC2) and properly selecting and tweaking these parameters are necessary to achieve reliable binding free energy estimations in computational investigations [144]. The MM-GBSA module in Prime was utilized to evaluate the binding free energy (Gbind) of the docked complex. The binding free energy was determined using the VSGB solvent model, OPLS 2005 force field, and rotamer search methods [145]. The total free energy binding was determined using the following equation.

$$dGbind = Gcomplex - (Gprotein + Gligand)$$

2.2.2 ADME, and toxicity:

The online tool swissADME were used to anticipate the ADME parameters of PEs [146], and toxicity properties and drug likeness of PEs were predicted by preADMET. The Lipinski rule of 5 and swissADME was used to investigate the selected compound drug likeness properties.

2.2.3 Cell culture:

The breast cancer cell lines were acquired from NCCS Pune, India, and the cells were maintained at 37 ℃ with 5% carbon dioxide and humidity (90%) in growth media DMEM (catalog #AL219A, HI-Media) containing growth supplement (10% FBS and antibiotics).

2.2.4 Cell viability assay:

The anticancer activity of coumestrol against breast cancer cells (MCF-7, MDAMB-231) was studied by MTT assay. Briefly, 1×10^4 cells in each well were cultured on 96-well plates and allowed grow overnight. Further, the cells were treated with phytoestrogen at different concentrations for 24 h. Then, the cells were incubated for 2 h with 10 µL of 12 mM MTT solution in the dark condition. Media was removed and 100 µL of SDS in hydrochloric acid was added to dissolve the formed formazan crystals. Finally, the absorbances were recorded at 570 nm using multimode reader (Thermo Fisher Scientific, Waltham, Massachusetts, USA).

2.2.5 Colony formation assay:

The effect of coumestrol on rate of cell proliferation was studied using colony formation assay. MCF-7 and MDAMB-231 cells were seeded in 6-well plates (1×10^3 cells/well) and treated with either coumestrol (46 µM and 48 µM), EX527 (50 µM), or

DMSO for 24 h. After 24h, media was removed, cells were washed twice with PBS solution, fresh media was added to the wells, and incubated for two weeks. After the incubation period, the generated colonies were fixed by 70% methanol. Further, cells were stained with 0.5% w/v crystal violet and excess dye was removed by washing with distilled water and the resulted colonies were counted and analyzed using OpenCFU software.

2.2.6 Quantification of the intracellular ROS levels:

Intracellular ROS level was quantified by performing FACS analysis using 2'-7', Dichlorodhihydrofluroscein diacetate (DCFDA, Invitrogen, C2938). Approximately, 3×10^4 cells/well were seeded into a 6 well plate and cultured in DMEM with 10% FBS. Then treatment of cells with coumestrol for both cell line (46 and 48 μM) was carried out. The cells treated with H2O2 (100 μM) were taken as positive control. After the 24 h treatment, 25 μM DCFDA in Phosphate buffer saline solution treatment of cells for 30 min at 37 °C was carried out, then cells were trypsinised using 0.05% Trypsin-EDTA, resuspended with fresh media and directly analyzed by flow cytometer at 488nm (cytoFLEX, Beckman Coulter, USA).

2.2.7 Western blotting:

Breast cancer cells were treated with coumestrol (46 and 48 μM) for 24 h and total cell lysate protein was collected. 50 μg of protein sample was run on SDS-PAGE, after completion of gel run, protein gels were transferred to PVDF membrane. The protein blots were exposed to 5% fat dried milk powder for specific binding of antibody. Blots were incubated with Primary antibody (Catalog #NBP-1-4954065) overnight at 4°C. After that, blots were treated with specific horseradish peroxidase-labeled secondary

antibody at room temperature for 1 h. Finally, the blots were visualized using a chemiluminescence agent and developed by Bio-Rad ChemiDoc system.

2.2.8 Statistical analysis:

ANOVA was used to perform statistical analysis using GraphPad Prism (version 5.01, GraphPad Software Inc.). The results were represented as mean standard deviation and P-values indicate significance levels (*P ≤ 0.05, **P ≤ 0.01, ***P ≤ 0.001).

2.3 Result and Discussion:

2.3.1 Molecular docking of phytoestrogens with human sirtuins:

We performed multi-molecular docking studies of natural plant-derived molecules, phytoestrogens (PE), with human sirtuins of sirtuins 1-3, which are the significant SIRTs that are involved in the majority of cancers, including breast cancer. From the molecular docking, we obtained the binding energies of PEs that bind to SIRTs proteins 1-3 (supplementary) and identified the possible target-specific PE molecules, which are discussed below:

2.3.2 Binding to sirtuins (1-3):

Sirtuin expression varies according to the stage of breast cancer. According to earlier research studies, different sirtuins play diverse roles in the development and spread of breast cancer [147].

2.3.2.1 SIRT-1 Binding:

SIRT-1, the first sirtuin identified, belonging to a class III histone deacetylase enzyme, localized in the nucleus, depends on nicotinamide adenine dinucleotide (NAD+) for its catalytic activity [148]. Upregulation of SIRT-1 directly impacts various aspects

of tumor development, including progression, metastasis, tumor cell apoptosis, autophagy, DNA repair, and other interconnected mechanisms involved in tumorigenesis [149]. In this study, we examined the PEs interaction profile at active site of SIRT-1 protein, the obtained results were compared with reference inhibitor EX-527. Our docking studies showed binding energies of PEs, amongst all, coumestrol showed higher binding energy -10.9 kcal/mol at SIRT-1 active site. However, the binding energy of coumestrol was similar compare to standard inhibitor EX527 (-10.26 kcal/mol). The following active site residues like ASP 348, ILE 316, ILE 347, ILE 411, PHE 273, and PHE 297 were observed as similar to coumestrol at SIRT-1 active site. It seems that most of the binding pockets were occupied by a ligand similar to the standard EX527 SIRT-1 inhibition has shown significant potential in cancer prevention, including breast cancer, suggesting that SIRT-1 inhibitors could be important agents in cancer treatment [150-152]. Identified PEs specific binding to SIRT-1 further optimized in order to suppress the advanced breast cancer. The PEs ligand coumestrol showed hydrogen bonding with ASP 348 and VAL 412, also taking π-σ interactions with PHE 273 and PHE 297. ILE 316 and ILE 411 forms the π-alkyl interaction, while PHE 273 and PHE 293 forms the π–π interaction with ligand. EX527 displayed conventional hydrogen bonding with ASP348 and ILE347, while PHE 273 and PHE 297 forms the π-σ and π-π interaction. ILE 279 and ILE 316 showed the π-Alkyl interaction (Figure 6).

2.3.2.2 SIRT2 Binding:

SIRT2 is one of the sirtuins studied widely, has significant role in cellular aging, genome stability, and energy metabolism [153]. SIRT2 is mostly found in the cytoplasm and involved in tumorigenesis, DNA damage, cell cycle, and infection [154]. It has increased deacetylation activity towards a variety of substrates, including p53, FOXO, p65, and p300 [155, 156]. NPD11033 is specific SIRT2 inhibitor, therefore it was chosen

as the standard SIRT2 inhibitor in our docking study. From the docking, coumestrol showed the highest binding energy -9.85, kcal/mol for the SIRT2 were observed. The coumestrol displayed interaction with residues like ALA 135 and PHE 190 at binding site of SIRT2 and interaction amino acids were similar to standard NPD11033 (-11.19 kcal/mol). For the SIRT2 protein, coumestrol forms the conventional hydrogen bonding with ASP 170 and PHE 131, while PHE 190 and LEU 134 showed π-π interaction, as well as π-σ interaction with ALA 135. NPD11033 forms the π-π interaction with PHE 96 and PHE190 and also showed π-alkyl interactions with ALA 135, ILE 169 with the ligand (Figure 6).

2.3.2.3 SIRT3 Binding:

SIRT 3 is predominantly expressed in mitochondria, Where it modulates the global proteins by maintaining the metabolic adaptation [157]. It is also involved in the regulation of reactive oxygen species (ROS) by avoiding the formation of abnormally high ROS levels to support the coordination of metabolic and genetic processes [158]. Additionally, SIRT3 mutation accelerates the development of chronic conditions such as cancers, cardiovascular problems, and neurological diseases [159]. Docking results showed, coumestrol has high binding energies -9.55 kcal/mol. The ligand coumestrol formed interaction with residues such as ALA 146, ASP 156, ILE 230 and PHE 157 were observed at SIRT3 site and type of interaction was similar as to the EX-A3489 (-10.73 kcal/mol). In case of SIRT3, coumestrol made conventional hydrogen bonding interactions with ALA 146, ILE 230, PHE 147 and TYR 165. Similarly, ASP 156, ASN 229 and SER 149 undergo carbon-hydrogen interactions with the ligand. EX-A3489 also forms the carbon-hydrogen interaction with ASP 156, GLN 228 and SER 149 and it also shows π-σ interaction with ALA 146. PHE 294 forms the π-alkyl interactions with ligand

(Figure 6). Further, we performed docking studies using another two algorithms (Autodock vina and Schrödinger) and results were included in the supplementary data.

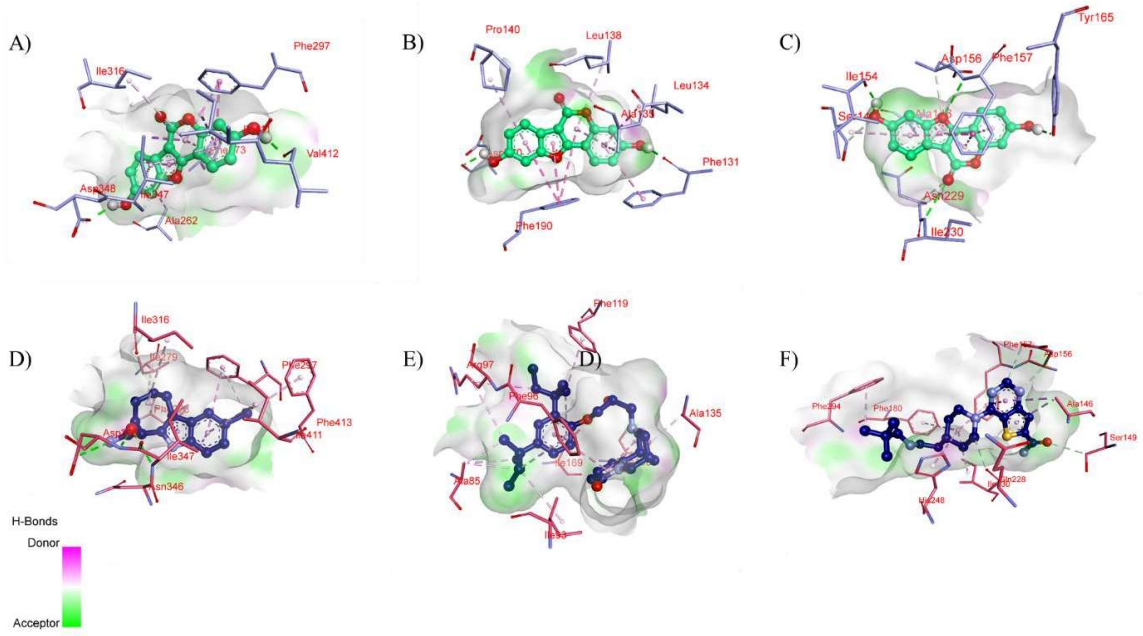

Figure 6: Binding interaction of COU and standards at SIRT-1-3 active sites. A) and D) were interaction of SIRT-1 with COU and EX527, B and E were interaction of SIRT2 with COU and NPD11033, and C) and F) were interactions of SIRT3 with COU and EX-A3489. (COU: Coumestrol; SIRT: Sirtuins).

2.3.3 ADME and toxicity parameters:

According to Lipinski's rule of five, the charge, hydrogen bonding, molecular weight, lipophilicity and polar charge were the five important properties to optimize to improve BBB transport [160]. ADME prediction provided by the preADMET server showed that the selected compounds follow the Lipinski's rule of five.

Further, we observed human intestinal absorption (HIA) of selected compound, it has highest HIA value around 97.50% suggests significant absorption capability. It was

found that the BBB binding and permeation ratio of this compound is greater than 0.1 (0.71) suggesting it has more CNS penetration and binding is considered active. It also exhibits the maximum PP binding, inhibitory effect to CYP 2_C19, CYP_3A4 enzymes (supplementary). The selected compound was predicted as non-carcinogenic to both mice and rat (supplementary).

2.3.4 Molecular dynamics:

To carry out their essential functions, proteins interact dynamically with other proteins, tiny molecules, and biopolymers. Molecular dynamics (MD) simulations provide comprehensive insights into the movement and path taken by molecules while interacting with other molecules [161]. MD facilitates the analysis of several possible connections and conformational changes within a system. And also helps in analysis of molecular solvation, protein structural traits, and drug-protein interactions. In this study, the ligand coumestrol outline of stability and possible interactions with proteins SIRT-1, -2, and -3 were studied through MD simulations and compared with references compounds.

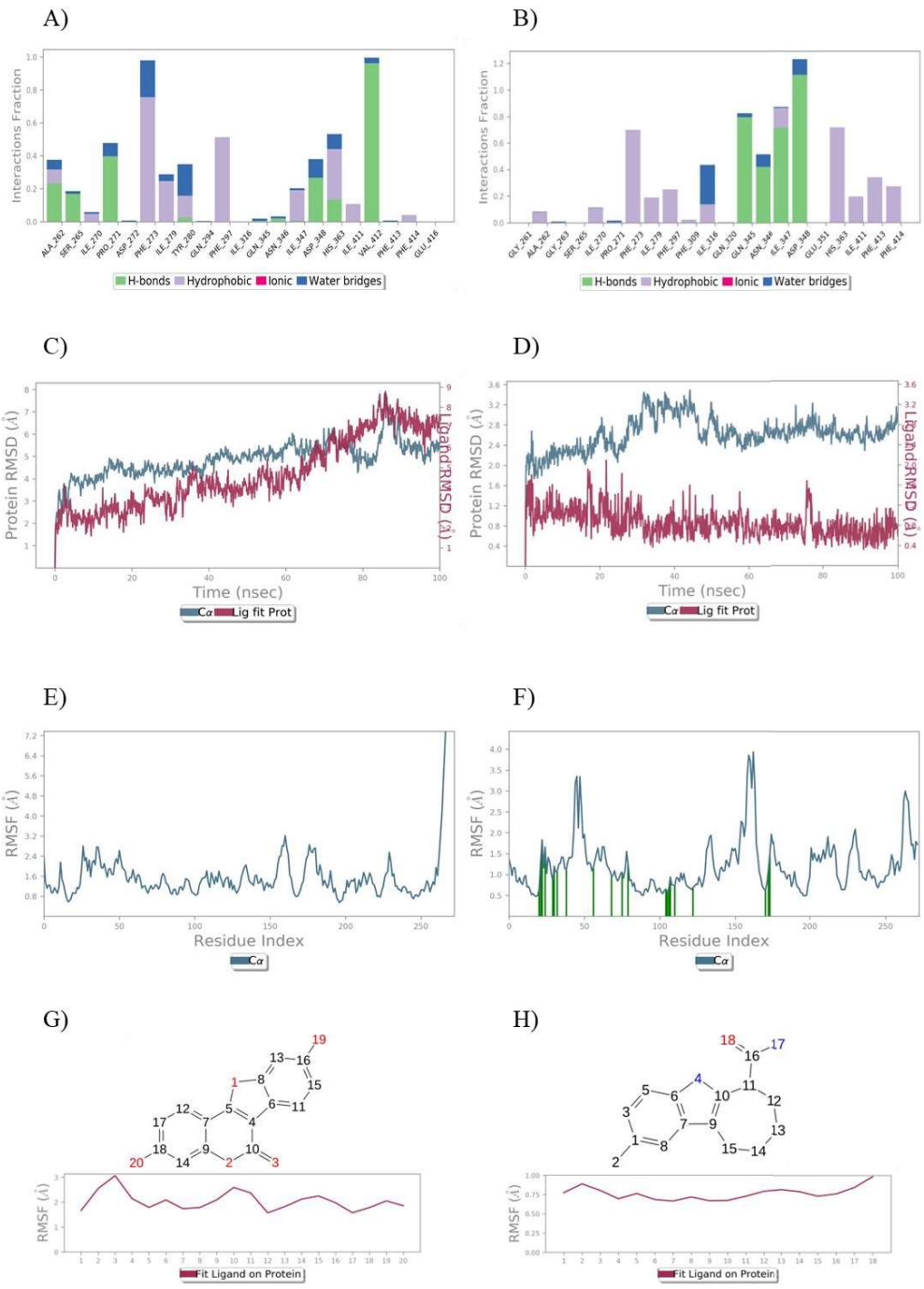

Figure 7: Coumestrol modulates the SIRT-1 interaction on molecular dynamics: A) bar charts of ligand-protein interactions, B) bar charts reference ligand-protein interaction, C) RMSD of ligand COU at active site, D) RMSD of reference ligand at active site, E) and G) RMSF plot of protein SIRT-1, F) and H) RMSF plot of reference

protein SIRT-1 (COU; Coumestrol, RMSD; root mean squire deviation, RMSF; root mean squire fluctuation).

The SIRT-1 protein and ligand interaction were better understood by the protein ligand bar diagrams Figure 7A. From the protein and ligand interactions, Coumestrol showed hydrogen bonding with ALA262, SER265, PRO271, ASP348, HIS363 and VAL412, hydrophobic bonds with PHE273, HS279, TYR280, PHE297, HE347 and HE411. No ionic interactions were observed. Further, we analyzed the SIRT-1 protein with coumestrol of Root mean square deviation (RMSD) and root mean square fluctuation (RMSF), was analyzed up to 100ns. We observed that RMSD of protein below 3°A, although there were slight fluctuations were noted between 0 to 20ns. The protein ligand complex RMSD trajectory further demonstrated that the ligand successfully diffuses into the binding site (Figure 7). We observed little high RMSD values for coumestrol it indicates a significant degree of ligand flexibility within the SIRT-1 active site. The observed instability can be attributed to the flexibility that allows coumestrol to explore many binding positions. Coumestrol may interact with water molecules, when exposed to a solvent environment; this might disrupt the binding of the compound and raise the RMSD readings.

For SIRT2, protein-ligand interaction, Coumestrol displayed hydrogen bonding with PHE96, PHE143 and ASP170, following hydrophobic bonds with ALA135, LEU139, PRO140, ASN168, HBS167 and PHE190. The RMSD and RMSF of protein-ligand were analyzed and were in optimal range up to 100ns (Figure 8). In case of SIRT3, coumestrol forms the hydrogen bonds with ILE154, PHE157, LEU164, HIS248 and VAL324, followed by hydrophobic bonds ASP156, GLU177, ALA247, PHE293, and GLU323. The protein-ligand RMSD and RMSF were analyzed up to 100ns and

illustrated. Subsequently, the protein and ligand trajectory of both SIRT2 and SIRT3 of ligand disseminates at binding pockets (Figure 9). For ligand binding and stability, hydrophobic pocket formation and hydrogen bond interactions are crucial in the active sites of SIRT-1, SIRT-2, and SIRT-3. The hydrophobic and hydrogen bonding interactions that coumestrol uses to engage at these sites vary depending on the SIRT and impact the binding stability and affinity of the drug. Variations in RMSD and binding stability seen in computational studies can be explained by analyzing these interactions, which also shed light on the binding kinetics.

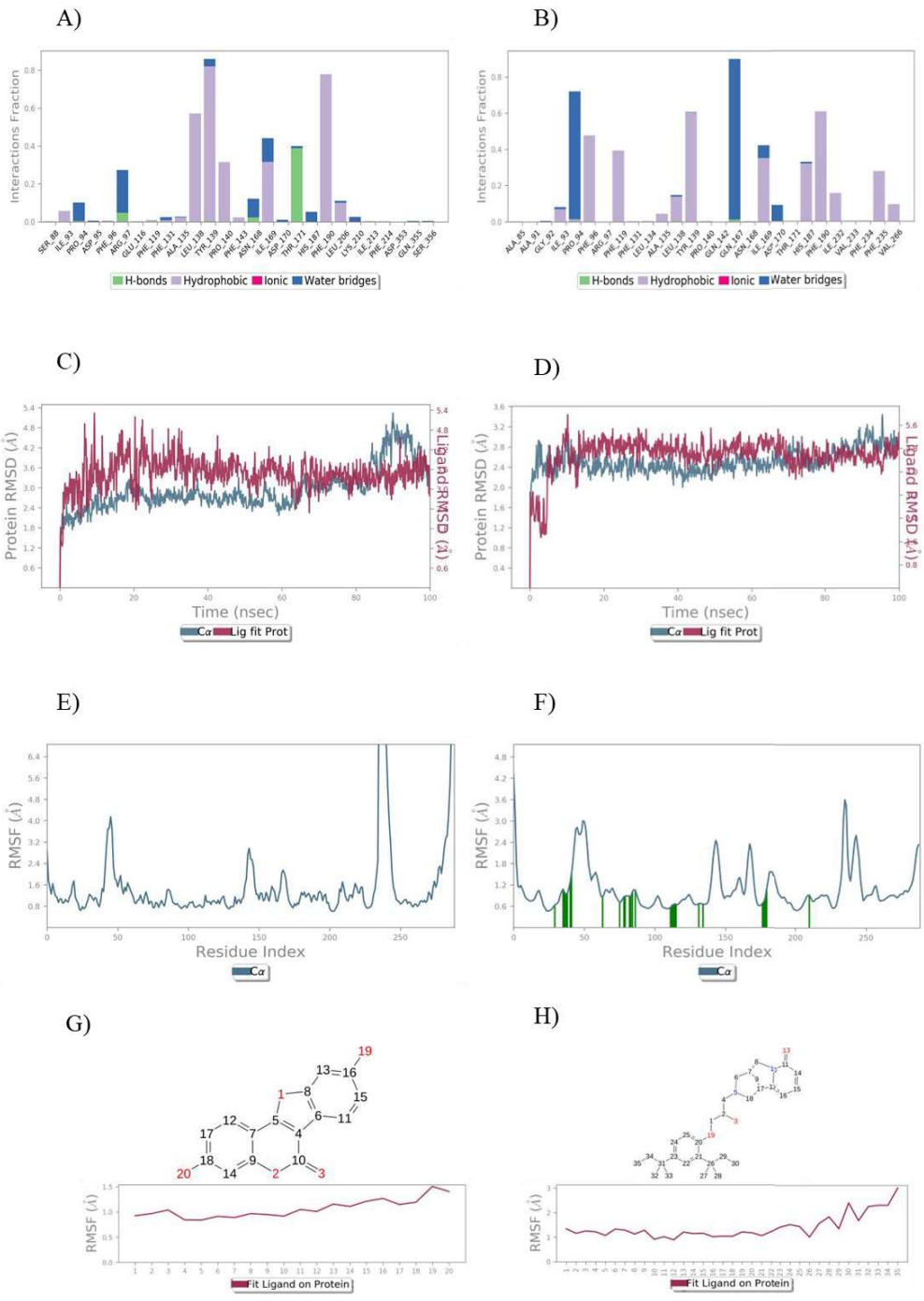

Figure 8: COU modulates the SIRT2 interaction on molecular dynamics: A) bar charts of ligand-protein interactions, B) bar charts reference ligand-protein interaction, C) RMSD of ligand COU at active site, D) RMSD of reference ligand at active site, E) and G) RMSF plot of protein SIRT2, F) and H) RMSF plot of reference protein SIRT2

(COU; Coumestrol, RMSD; root mean squire deviation, RMSF; root mean squire fluctuation).

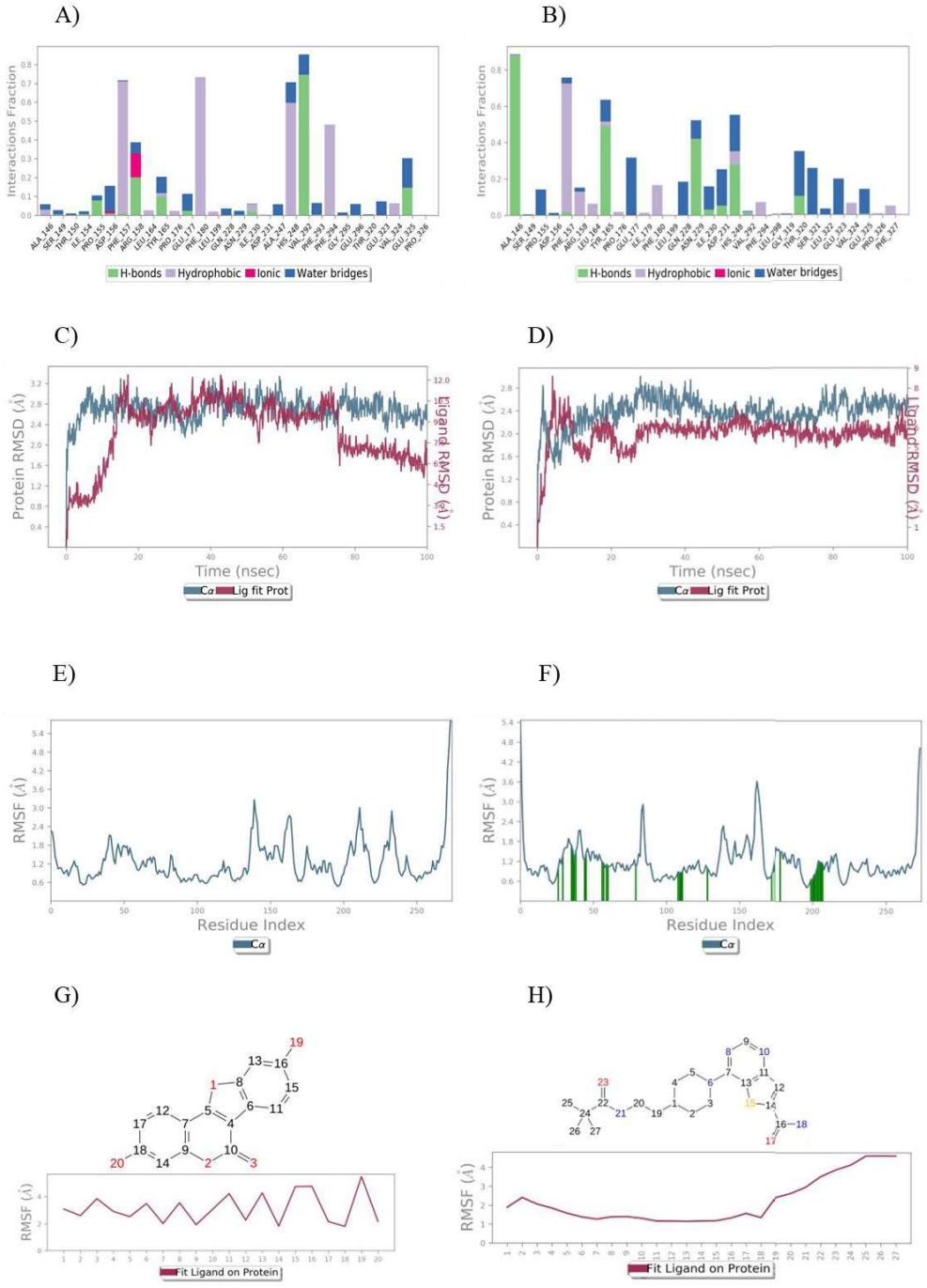

Figure 9: COU modulates the SIRT3 interaction on molecular dynamics: A) bar charts of ligand-protein interactions, B) bar charts reference ligand-protein interaction,

C) RMSD of ligand COU at active site, D) RMSD of reference ligand at active site, E) and G) RMSF plot of protein SIRT3, F) and H) RMSF plot of reference protein SIRT3 (COU; Coumestrol, RMSD; root mean squire deviation, RMSF; root mean squire fluctuation).

Reliable molecular modelling depends on the precise measurement of protonation states for residues in the ligand binding site. Validation of the protonation states accurately reflect physiological circumstances and the unique binding site environment by combining pKa prediction techniques, empirical data, and simulation validation. The binding energy of ligands to protein molecules is commonly assessed using the MM-GBSA technique. The impact of extra non-bonded interaction energies and each SIRTs - Coumestrol complex's binding free energy were assessed. The binding energies of ligand to SIRT-1, 2, and 3 are -52.26, -72.93, and -67.62 (kcal/mol). GbindCoulomb, GbindvdW, and GbindLipo are the key determinants of average binding energy for all kinds of interactions. Consequently, the MM-GBSA estimates produced from the MD simulation trajectories provided strong support for the binding energy acquired from the docking data (Table 1).

Table 1: Average MM-GBSA binding energy calculation of coumestrol with SIRT-1, 2, and 3 from MD Simulation trajectories.

Energies (kcal/mol)	**Coumestrol**			**Reference Compounds**		
	SIRT-1	SIRT2	SIRT3	SIRT-1 (Ex-527)	SIRT2 (NPD11033)	SIRT3 (EX-A3489)
dG_{bind}	-52.26373207	-72.93049833	-67.62823825	-62.25673227	-79.93029537	-57.62326829
dG_{bind}Lipo	-16.88376881	-33.61948827	-18.31760711	-19.88379683	-39.21349827	-16.39730213
dG_{bind}vdW	-38.48624483	-61.4374613	-58.69295482	-36.78675464	-68.23946353	-55.99293278
dG_{bind}Coulomb	-16.7859367	-0.134873755	-13.92917175	-18.24867237	-12.134673565	-17.82935179
dG_{bind}Hbond	-2.562772239	0	-1.984817482	-4.763853319	-2.364569872	-2.898681526
dG_{bind}Packing	-2.304582456	-0.983341073	-5.396111795	-4.668958278	-2.782653076	-6.256123624

2.3.5 Effect of Coumestrol on cell proliferation:

MTT assay was performed to investigate the effect of coumestrol on cell proliferation in breast cancer cell lines. Coumestrol (5, 10, 20, 40, 80 and 160 µM) were treatment of the breast cancer cell lines for 24 h as per the standard protocol [162]. From the MTT assay, the percentage cell viability of breast cancer was illustrated (Figure 10). Further, we measured half maximal growth concentration of coumestrol in MCF-7 and MDAMB-231 and was found to be 46 µM and 48 µM, respectively. Additionally, we observed coumestrol effect on cell morphology in breast cancer cell line, it showed change in morphology of cells upon treatment with coumestrol suggesting that coumestrol has antiproliferative activity.

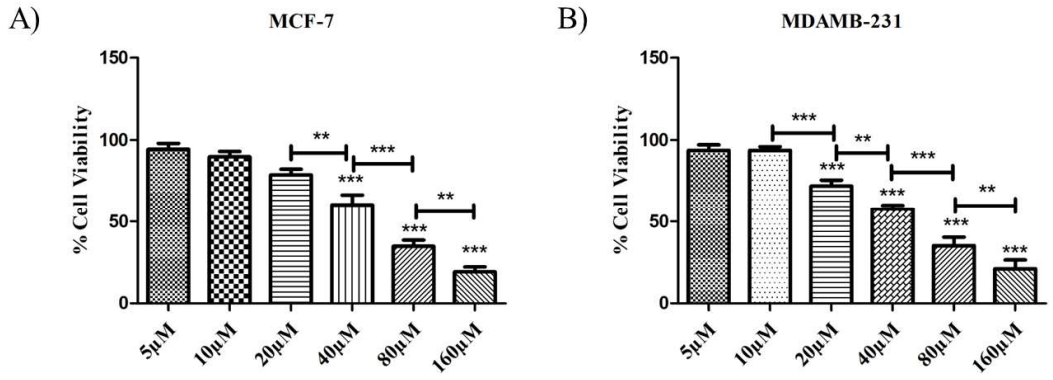

Figure 10 : COU impacts the cell viability of breast cancer cells. A, B) Percentage cell viability of MCF-7 and MDAMB-231 treated with coumestrol (5-160 µM) (± SD, n = 3 [*P < 0.05, **P < 0.01, ***P < 0.001]), (COU; coumestrol).

2.3.6 Effect of Coumestrol on colony formation:

We conducted the clonogenic assay to confirm the long-term impact of COU on the stemness property and cell proliferation of breast cancer cells. COU showed the reduction in formation of colony in both the breast cancer cell lines, shown in Figure 11. Additionally, when compared to the control group, we noticed COU treatment declined

the colony formation. Further we analyzed the survival fraction (%) highlighting the reduced cell survival upon COU treatment. It suggests, COU inhibits the colony formation showing long-term effect on breast cancer cell line.

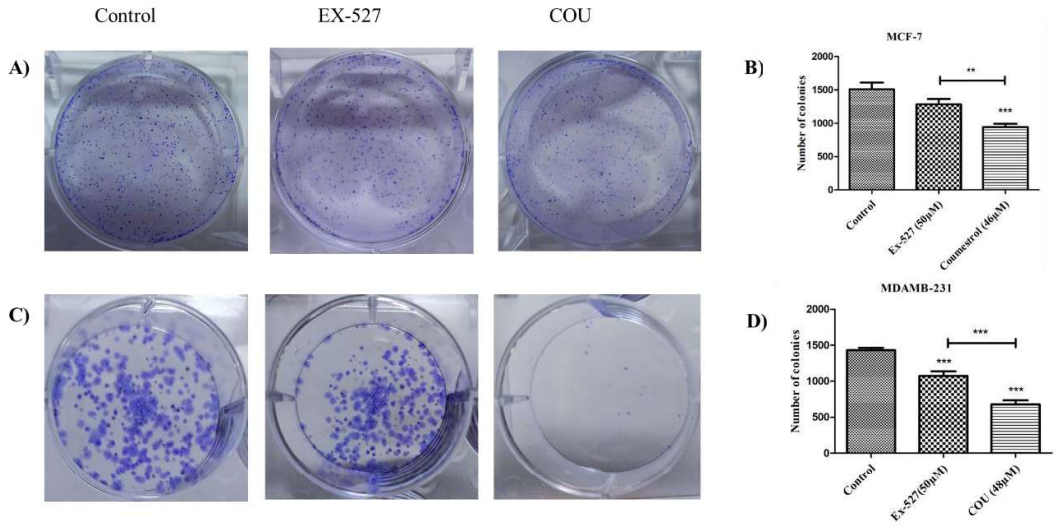

Figure 11: COU reduces colonies in breast cancer cells. A), MCF-7 cells were treated with or without COU (46 μM), EX-527 50 μM for 24 h B), Number of colonies average plotted against drug concentrations in MCF-7 cells. C) and D), MDAMB-231 cells were treated with or without COU (48 μM), EX-527 50 μM for 24 h and average number of colonies plotted against drug concentrations in MDAMB-231 cells (COU; coumestrol) (± SD, ANOVA where, n = 3 [*P < 0.05, **P < 0.01, ***P < 0.001]).

2.3.7 Effect of Coumestrol on intracellular reactive oxygen species:

SIRT-1 inhibits the ROS generation through regulating the expression of cellular antioxidant genes [163]. The induction of ROS production, decreased metastasis, and decreased cellular viability in breast cancer cells are all associated with persistent SIRT3 suppression [164]. To investigate the effect of COU on reactive oxygen species, we measured the intracellular reactive oxygen species by performing FACS analysis in breast cancer cell line. COU induces ROS generation in both breast cancer cell lines, when

compared with well-known ROS inducer, hydrogen peroxide. The results showed that COU induces ROS cellular levels by 67% and 74% in both cell lines, whereas, hydrogen peroxide caused 94% and 89% of ROS levels (Figure 12).

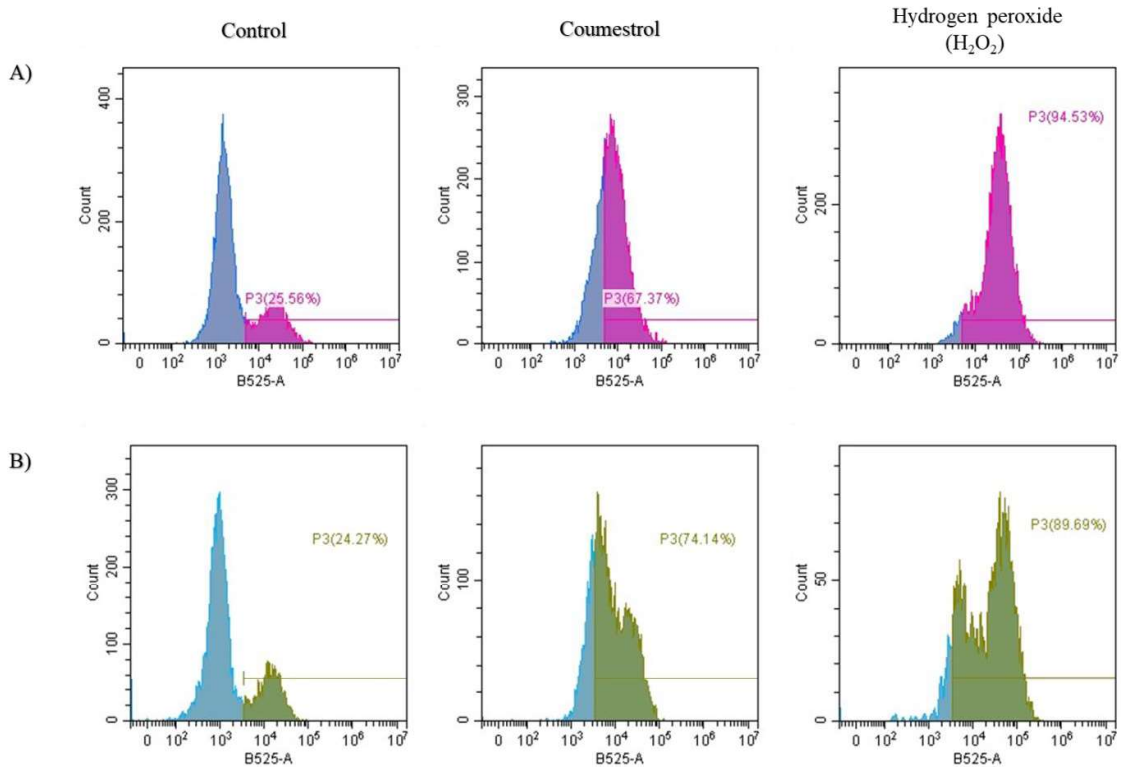

Figure 12: Effect of COU on intracellular ROS in breast cancer cell lines: A), intracellular ROS levels of control, COU (46 µM) and hydrogen peroxide (100 µM) in MCF-7 cells B), intracellular ROS levels of control, COU (48 µM) and hydrogen peroxide (100 µM) in MDA.

2.3.8 Effect of Coumestrol on SIRT inhibition:

To confirm the results of docking and MD studies, we assessed whether COU induces sirtuin inhibition. The breast cancer cells were treated with 46 µM and 48 µM COU for 24 h, and SIRT-1 protein expression levels were examined using western blotting as shown in Figure 13. Results indicated that COU significantly reduced the level

of SIRT-1 protein expression compare to control in MCF-7 and MDAMB-231 breast cancer cell lines at 24 h with half minimal dose (Figure 13).

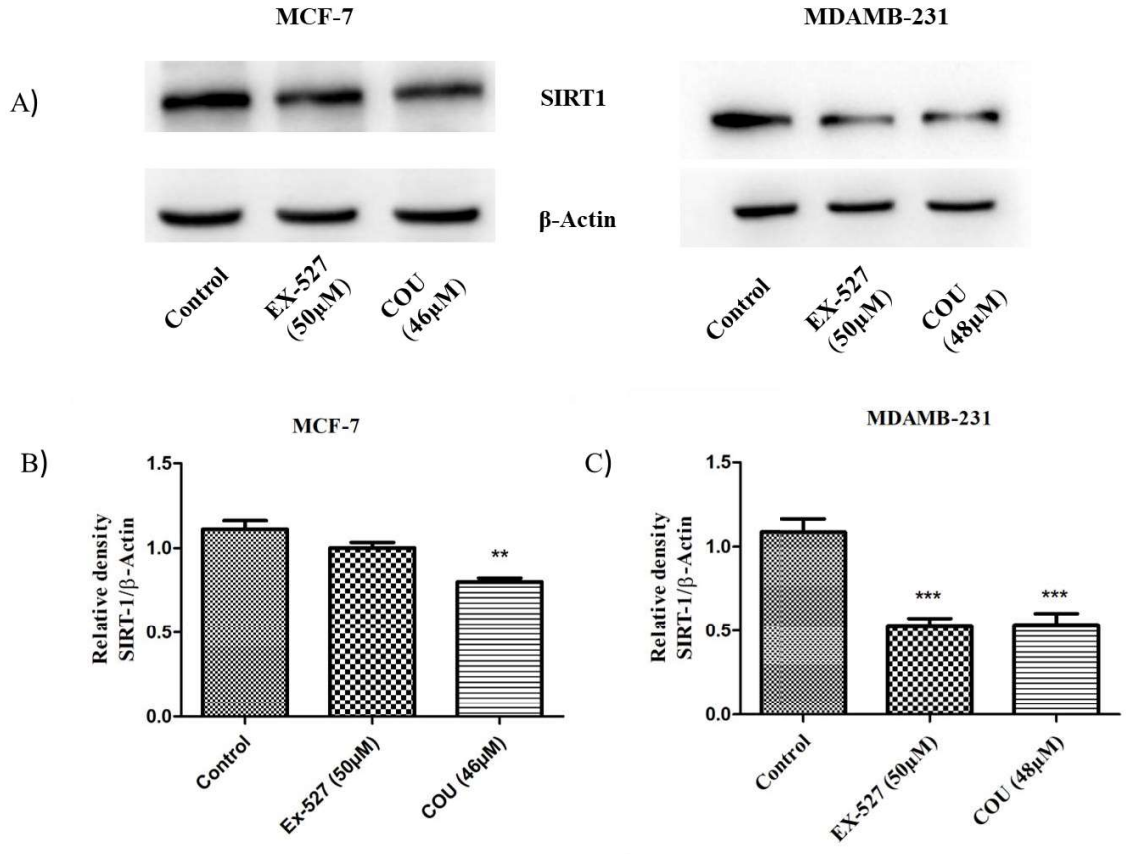

Figure 13: COU induces sirtuin inhibition. A) Expression of SIRT-1 protein was detected by western blotting. (B, C) Relative density of SIRT-1 protein against β-actin was quantified using ImageJ software (COU; coumestrol) (± SD, ANOVA [*P < 0.05, **P < 0.01, ***P< 0.001])

The substantial activity of COU against various SIRTs, with particular emphasis on SIRT-1, SIRT-2, and SIRT-3 was found to be in promise with the combined results from in vitro and in silico studies. Fascinatingly, in silico results suggested that the lead compound had potential ADMET (Absorption, distribution, metabolism, excretion, and toxicity) characteristics, and our in vitro results showed that COU has a significant

amount of potency against its particular target. Overall, in vitro and in silico results are consistent, indicating that coumestrol can be further studied as possible sirtuin inhibitors. It can be investigated individually or in combination with anticancer drugs to prevent and lag the breast cancer progression to avoid the emergence of cancer drug resistance.

The present study employed relevant in vitro and in silico techniques primarily focusing on proving the concept that coumestrol imparts anticancer activity through sirtuin inhibition. However, further studies are required to unravel the drug and protein target interactions with physiological considerations using surface plasmon resonance (SPR), bio-layer interferometry (BLI), or cellular thermal shift assay (CETSA) techniques.

2.4 Conclusion:

In conclusion, the current study demonstrated and investigated phytoestrogens sirtuins binding and its anticancer activity against breast cancer. The *in-silico* studies determine the most effective binding agents with sirtuins. Further, MD studies revealed protein ligand stability of phytoestrogen with sirtuins. The results showed, phytoestrogens involve in sirtuin binding, decrease in the cell viability of human breast cancer cells and induce cellular ROS level, reduce formation of colonies and inhibit the sirtuin protein expression levels. Overall, phytoestrogens were proven as an anticancer agent and effective sirtuin inhibition observed in breast cancer cells. which can be considered for further studies as potential chemotherapeutic drugs to improve clinical outcomes.